Earthquake Engineering, Tenth World Conference © 1992 Balkema, Rotterdam. ISBN 90 5410 060 5

Embedment effects on dynamic soil-structure interaction

Y.Ohtsuka & A.Fukuoka
Kajima Corporation, Tokyo, Japan

E.Yanagisawa
Tohoku University, Miyagi, Japan

H.Fukudome
Nuclear Power Engineering Center, Tokyo, Japan

ABSTRACT: Forced vibration tests for large scale models of embedded structures with different embedment depths were performed to investigate response characteristics and to provide data for verification of analysis codes. The test results indicated that the response characteristics of the embedded structures were significantly affected by the backfill and surrounding soil. The analysis codes, Sway-Rocking model and Axisymmetric Finite Element Method, were confirmed to be applicable for evaluating the embedment effects on structure response.

1 INTRODUCTION

Structure response during an earthquake is greatly affected by soil-structure interaction. For embedded structures, even more complicated interaction will occur because of the existence of backfill and surrounding soil. In this study, forced vibration tests on large scale models on actual soil were performed to evaluate the embedment effects on structure response. The test model was scaled down to about 1/10 in consideration of the fundamental vibration characteristics of a BWR-type reactor building in Japan. The responses of the structure, backfill and surrounding soil including earth pressures at the bottom and the sides of the basement were measured, and the dynamic soil impedance functions are discussed. In the correlation analyses, the following two analysis codes are used (1) the Sway-Rocking model, hereafter called the "S-R" model, employing the soil impedances of the bottom determined by the three dimensional wave propagation theory in layered soil and the side impedances calculated by Novak's method, and (2) the Axisymmetric Finite Element Method, hereafter called the "FEM" model.

2 TEST RESULTS

2.1 *Test conditions*

Two RC test model structures named Model A and Model B were constructed about 60m apart on a soft rock site. A general view of Model B is shown in photograph 1 and a cross section of Models A and B is shown in Figure 1. Model A has an 8m-square basement weighing about 450 ton and the total height of 5m. Model B has an underground structure with the same dimensions as Model A and a 5.5m-high two-storied superstructure erected on the underground structure. The total weight of Model B is about 657 ton.

Sinusoidal forced vibration tests were performed on the two models for different embedment depths,

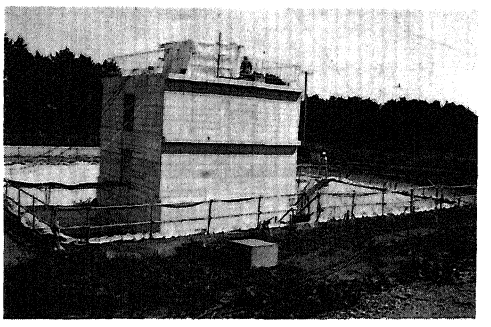

Photograph 1. Test model B

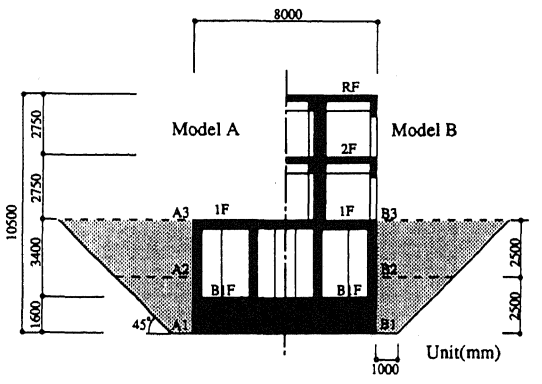

Figure 1. Cross section of test models

namely A1 and B1 (non-embedment), A2 and B2 (half-embedment;2.5m) and A3 and B3 (full-embedment;5.0m), by a vibration exciter installed on the first floor (1F) of the test models. In the case of Model B, excitation at the top floor (RF) was also carried out for each embedment depth.

The responses of the test models, the backfill soil and

the surrounding soil, and the earth pressures at the foundation bottom and the side wall of the embedded foundation were measured.

2.2 *Response of test models*

Figure 2 shows the resonance frequency and critical damping factor for each test corresponding to embedment depth. It is confirmed that these values increase with increasing embedment depth for both models.

The displacement ratios of the test models at the resonance frequencies are summarized in Figure 3. Model A vibrated as a rigid body. Its displacement ratios of sway and rocking to top horizontal displacement hardly change with embedment depth. The sway and rocking ratios in the displacement at RF for Model B for RF excitation are not sensitive to embedment depth, but the ratio of elastic deformation of the superstructure increases with increasing embedment depth. For 1F excitation, the rocking ratio decreases and the ratio of elastic deformation increases with increasing embedment depth.

Figure 4 shows the horizontal displacement resonance curves at the foundation bottom for Model B for RF and 1F excitation. The peak amplitudes decrease and the resonance frequency shifts towards the high frequency with increasing embedment depth. The resonance curves for RF and 1F excitation have different characteristics except for the resonance frequency, and each resonance curve for 1F excitation has a dip in the vicinity of 13 Hz.

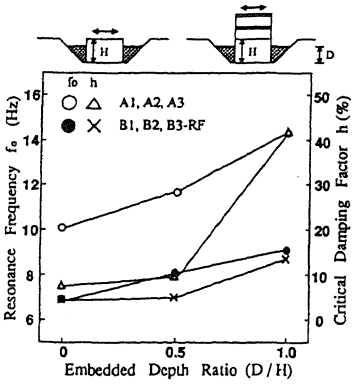

Figure 2. Resonance frequency and critical damping factor

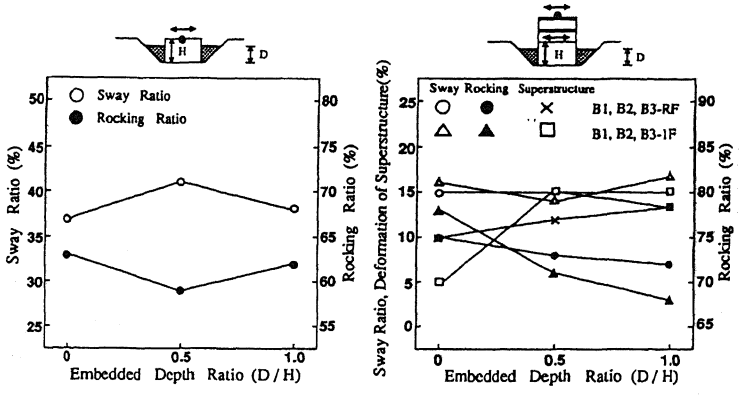

(a) A1, A2 and A3 tests (b) B1, B2 and B3 tests

Figure 3. Displacement ratios of test models at resonance frequency

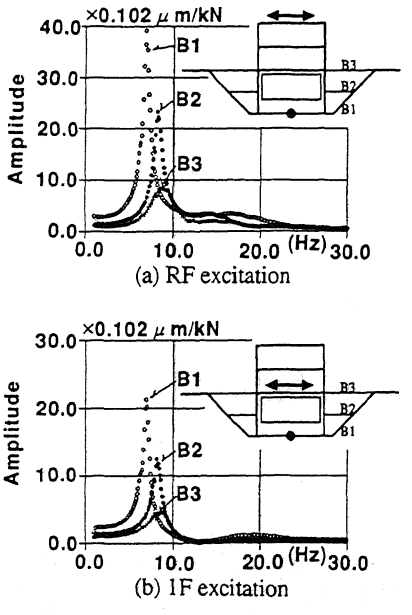

(a) RF excitation

(b) 1F excitation

Figure 4. Horizontal displacement resonance curves at foundation bottom

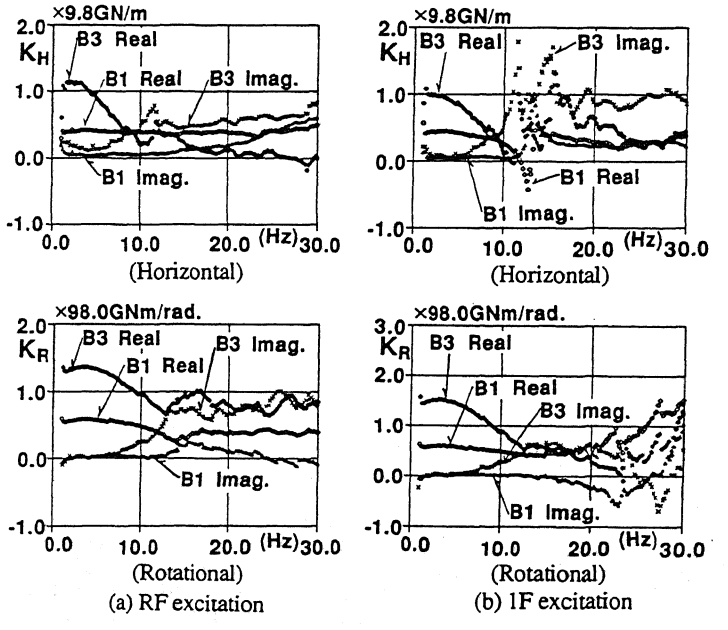

(a) RF excitation (b) 1F excitation

Figure 5. Comparison of combined soil impedances of B1 and B3 tests

2.3 *Soil impedances*

In this study, combined soil impedances derived from test results, and dynamic soil impedances, are expressed in the following formulas:

$$Q/u_0 = K_H = K_{HH} + K_{HR}\,\theta_0/u_0 \qquad (1a)$$

$$M/\theta_0 = K_R = K_{RR} + K_{RH}\,u_0/\theta_0 \qquad (1b)$$

where

u_0, θ_0 : Horizontal and Rotational displacements at Foundation Bottom (Test results)

Q, M : Shearing Force and Moment at Foundation Bottom

K_H, K_R : Combined Horizontal and Rotational Impedances

K_{HH}, K_{RR} : Dynamic Horizontal and Rotational Impedances

$K_{HR} = K_{RH}$: Dynamic Coupling Impedances

Figure 5 shows the combined horizontal and rotational soil impedances for tests B1 and B3 for RF and 1F excitation. The embedment effect is to increase the real and imaginary parts with increasing embedment depth and this complicates the dynamic characteristics. However, the combined soil impedances for RF and 1F excitation do not coincide, and the horizontal components for 1F excitation have large fluctuations around 12-15 Hz.

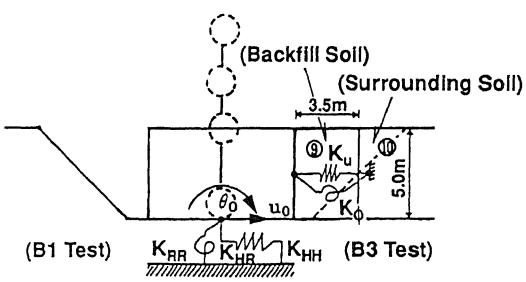

Figure 6. Sway-rocking model

These phenomena are due to differences in the contribution of the coupling component to the combined soil impedances.

3 CORRELATION ANALYSES

Many methods have been proposed for the analyses of the dynamic characteristics of embedded structures. Correlation analyses were carried out for the basement part, i.e., Model A (Miyamoto 1991). This paper describes the comparative investigations of test results for the RF excitation of Model B by the following two analytical techniques.

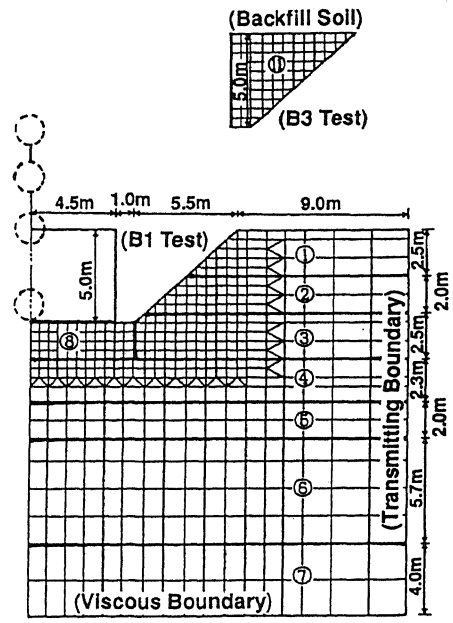

Figure 7. Axisymmetric FEM model

Table 1. Soil constants for analysis

(a1) S-R model(underneath foundation bottom)

Thickness of Layer (m)	Mass Density ρ(t/m³)	Shear Wave Velocity Vs(m/s)	Poisson's Ratio ν	Damping Factor h(%)
2.0	1.7	290	0.12	5
2.3	1.7	450	0.12	3
2.0	1.7	450	0.41	3
5.7	1.9	1330	0.11	3
–	2.1	1600	0.35	3

(a2) S-R model(at side wall of embedded basement part)

No.	Mass Density ρ(t/m³)	Shear Wave Velocity Vs(m/s)	Poisson's Ratio ν	Damping Factor h(%)
⑨	1.8	140	0.30	2
⑩	1.7	340	0.35	5

(b) Axisymmetric FEM model

No.	Mass Density ρ(t/m³)	Shear Wave Velocity Vs(m/s)	Poisson's Ratio ν	Damping Factor h(%)
①	1.5	140	0.39	5
②	1.7	270	0.29	5
③	1.7	340	0.34	5
④	1.7	450	0.12	3
⑤	1.7	450	0.41	3
⑥	1.9	1330	0.11	3
⑦	2.1	1600	0.35	3
⑧	1.7	270	0.12	5
⑪	1.7~1.8	110~150	0.30	2~4

3.1 *Analysis models*

In the correlation analyses, the (embedded) basement part is treated as a rigid body based on the measuring mode of the basement, and the structure is assumed as a multi-lumped mass model considering bending and shearing deformation.

For the evaluation of dynamic soil impedances, the following two analytical methods are applied:(1) the S-R model (Figure 6) and (2) the Axisymmetric FEM model (Figure 7). In the S-R model, the foundation-bottom soil impedances K_{HH}(horizontal impedance), K_{RR}(rotational impedance) and K_{HR}(coupling impedance) and the side-wall soil impedances K_u(horizontal impedance) and K_ϕ(rotational impedance) are calculated independently. The bottom impedances are defined assuming that the level of the foundation bottom is the ground surface, and calculation is executed using the three dimensional wave propagation theory in layered soil, while Novak's method considering the backfill soil and the surrounding soil is applied for the calculation of the side impedances. In the Axisymmetric FEM model, the energy dissipation from the analysis boundary of the finite soil towards the outside is evaluated with the addition of viscous damping at the bottom boundary and transmitting boundary at the side boundary. In these two analytical methods, the square basement is modeled as an equivalent circular basement, whose area is equal to that of the square basement. The constants of the soil properties adopted in these correlation analyses are summarized in Table 1. The element numbers in Table 1 ((a2) and (b)) are identical to those in Figures 6 and 7. These values are determined based on the measured data of the PS logging and the exploration with elastic waves at the test site.

3.2 *Soil impedances and resonance curves of displacement*

Figure 8 shows the comparison of the dynamic soil impedances. The soil impedances of test results K_{HH}, K_{HR}(=K_{RH}) and K_{RR} in equations (1a) and (1b) are evaluated from the data (K_H, K_R, u_0 and θ_0) for RF and 1F excitations using the method of least squares (Kobayashi 1991, Miyamoto 1991).

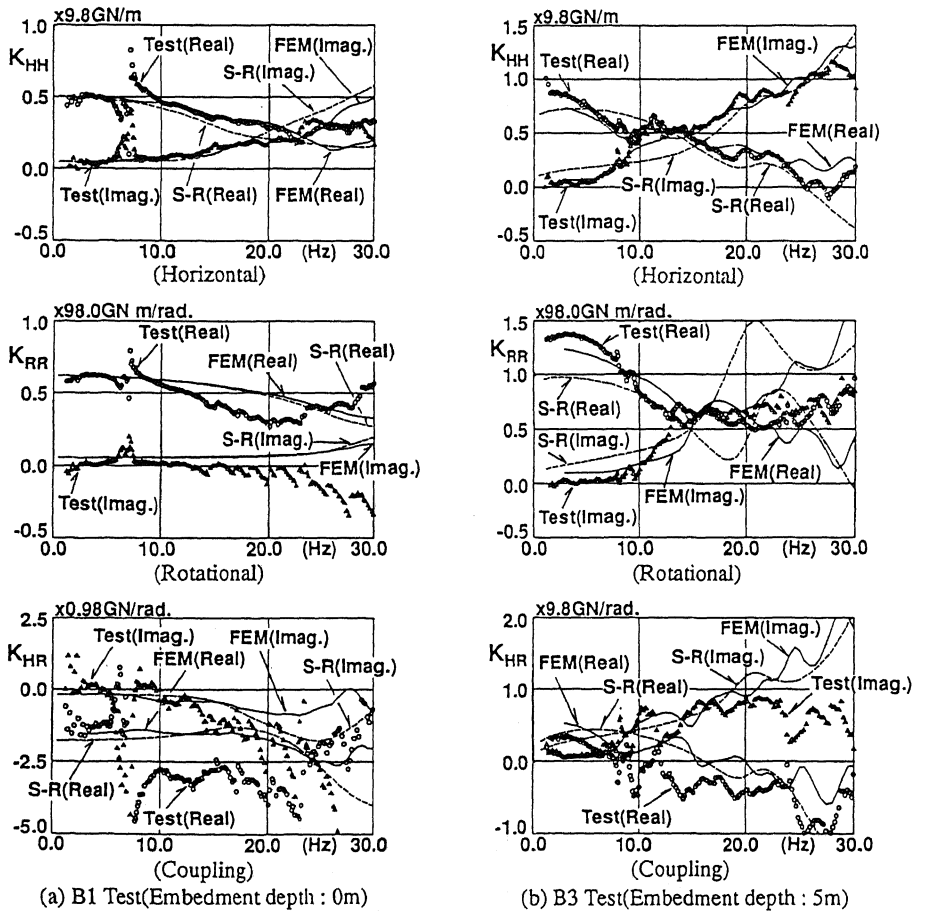

(a) B1 Test(Embedment depth : 0m)

(b) B3 Test(Embedment depth : 5m)

Figure 8. Comparison of dynamic soil impedances between tests and analyses

As shown in Figure 8(a), the analytical results by the two methods show good agreement with the test results, while the real part is underestimated in the higher frequency range by the S-R model. In the case of the embedded model, Figure 8(b), the analytical results by the S-R model conform approximately to the test results, while the real part is underestimated and the imaginary part is overestimated in the lower frequency range. It seems that these discrepancies between analytical results by the S-R model and the test results are caused by the assumption of two dimensional plane strain in the side impedances. The analytical results by the FEM model show good agreement with the test results, while differences are recognized between the analytical results and test results in the higher frequency range.

Figure 9 shows the comparison of the resonance curves at the RF and the 1F for the RF excitation. The analytical results of tests B1 and B3 show good conformity with the test results. The discrepancies of B3 test in the lower frequency range can be seen between the analytical results by the S-R model and test results.

3.3 *Resonance curves of earth pressure and acceleration*

Hereafter, the analytical results obtained by the axisymmetric FEM model will be adopted only as the comparison model with the test results.

Figure 10 shows the comparison of the resonance curves of vertical earth pressure at the foundation bottom in the horizontal excitation for RF. These test results show that the response amplitude increases at the border of the foundation bottom with similar frequency response characteristics to the displacement of the test structure. The analytical results show good agreement with the test results, while the amplifications of B3 test are underestimated around the first predominant frequency.

Figure 11 shows the comparison of resonance curves of the horizontal acceleration underneath the foundation bottom and the surrounding soil. The first predominant frequency of the acceleration of test results is in agreement with the resonance frequency of the test structure.

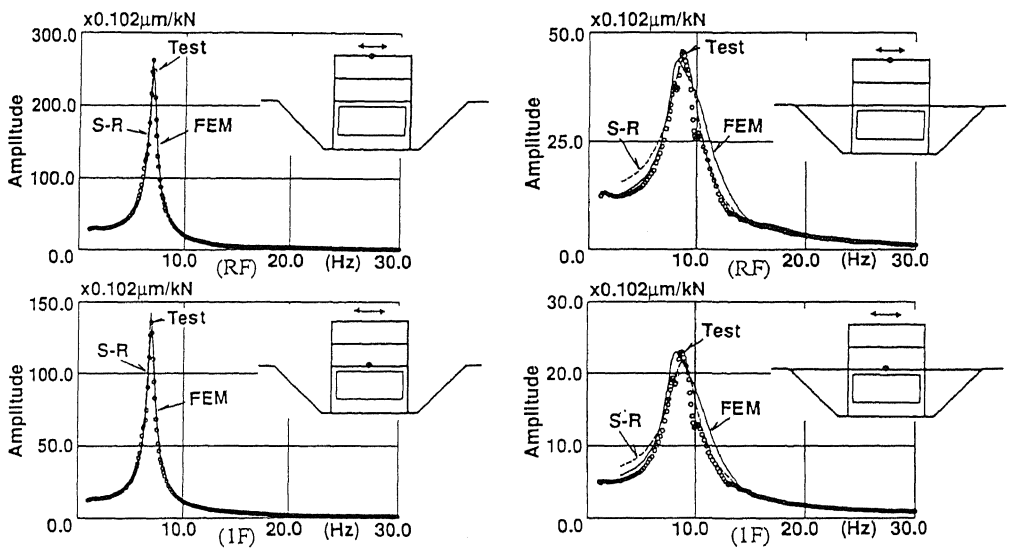

(a) B1 Test(Embedment depth : 0m)

(b) B3 Test(Embedment depth : 5m)

Figure 9. Comparison of horizontal displacement resonance curves at RF and 1F for RF excitation

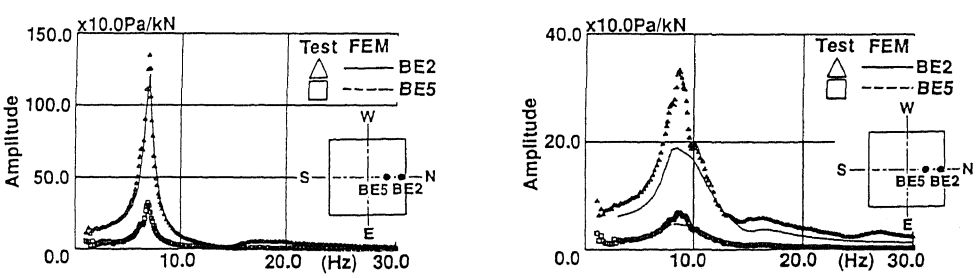

Figure 10. Comparison of resonance curves of vertical earth pressure at foundation bottom

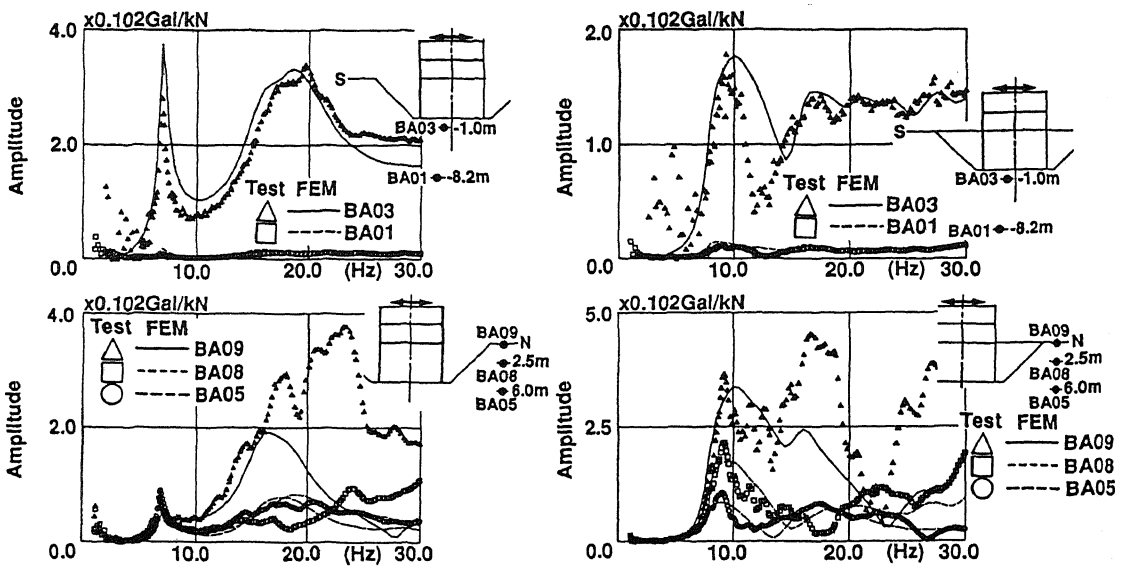

(a) B1 Test(Embedment depth : 0m) (b) B3 Test(Embedment depth : 5m)

Figure 11. Comparison of resonance curves of horizontal acceleration underneath foundation bottom and surrounding soil

The differences in resonance curve shape in the higher frequency range between tests B1 and B3 are due to the influence of backfill soil. As shown in Figure 11, the analytical results are in good agreement with the test results, while there is some discrepancy on the ground surface in the higher frequency range.

4 CONCLUSIONS

The investigations evaluated embedment effects on the structure response, and useful data were obtained from forced vibration tests to verify analysis methods. The concluding remarks of this study are as follows :

1.The real and imaginary parts of soil impedance increase with embedment depth and its dynamic characteristics become more complicated.

2.The structure-response amplitude decreases and the resonance frequency becomes higher with increasing embedment depth for the basement only as well as for the basement with the superstructure on it. For each embedment depth, the displacement ratios of sway and rocking to top horizontal displacement are similar in the basement only. For the basement with the superstructure on it, the ratio of elastic deformation of the superstructure increases with increasing embedment depth, but the sway component ratio is not sensitive to embedment depth.

3.The analytical methods used here, the S-R and Axisymmetric FEM models, can be adequately used to investigate the response characteristics of embedded basement-superstructures. In particular, the Axisymmetric FEM model is applicable for investigating frequency response characteristics of backfill soil and surrounding soil including earth pressures.

ACKNOWLEDGEMENTS

This work was carried out by NUPEC as an entrusted project sponsored by the Ministry of International Trade and Industry of Japan. This work is supported by the "Sub-Committee of Model Tests on Embedment Effect on Reactor Building" under the "Committee on Seismic Verification Test" of NUPEC. The authors wish to express their gratitude for the cooperation and valuable suggestions offered by the members of the Committee.

REFERENCES

Kobayashi, T., et al. 1991. Forced vibration test on large scale model on soft rock site (embedment effect test on soil-structure interaction). *Proc. 11th SMiRT*: Vol. K, 129-134.

Miyamoto, Y., et al. 1991. Experimental studies on an embedded structure-soil interaction. *Proc. 2nd International Conference on Recent Advances in Geotechnical Earthquake Engineering and Soil Dynamics*: Paper No.5.41, 845-852.